



LAWRENCE  
LIVERMORE  
NATIONAL  
LABORATORY

# X-ray Emission Spectroscopy of Cerium across The $\gamma$ - $\alpha$ Volume Collapse Transition

M. J. Lipp, A. Sorini, J. Bradley, B. Maddox, K. T.  
Moore, H. Cynn, T. P. Devereaux, Y. Xiao, P. Chow, W.  
J. Evans

July 6, 2012

Physical Review Letters

## **Disclaimer**

---

This document was prepared as an account of work sponsored by an agency of the United States government. Neither the United States government nor Lawrence Livermore National Security, LLC, nor any of their employees makes any warranty, expressed or implied, or assumes any legal liability or responsibility for the accuracy, completeness, or usefulness of any information, apparatus, product, or process disclosed, or represents that its use would not infringe privately owned rights. Reference herein to any specific commercial product, process, or service by trade name, trademark, manufacturer, or otherwise does not necessarily constitute or imply its endorsement, recommendation, or favoring by the United States government or Lawrence Livermore National Security, LLC. The views and opinions of authors expressed herein do not necessarily state or reflect those of the United States government or Lawrence Livermore National Security, LLC, and shall not be used for advertising or product endorsement purposes.

# **X-ray emission spectroscopy of cerium across the $\gamma$ - $\alpha$ volume collapse transition**

M. J. Lipp<sup>1</sup>, A. Sorini<sup>1,2</sup>, J. Bradley<sup>1,\*</sup>, B. Maddox<sup>1</sup>, K.T. Moore<sup>1</sup>, H. Cynn<sup>1</sup>, T.P. Devereaux<sup>2,3</sup>, Y. Xiao<sup>4</sup>, P. Chow<sup>4</sup>, W.J. Evans<sup>1</sup>

<sup>1</sup> *Lawrence Livermore National Laboratory, Livermore, CA 94550, USA*

<sup>2</sup> *Stanford Institute for Materials and Energy Sciences, SLAC National Accelerator Laboratory and*

*Stanford University, Menlo Park, California 94305, USA*

<sup>3</sup> *Geballe Laboratory for Advanced Materials, Stanford University, Stanford, California 94305, USA*

<sup>4</sup> *HPCAT, Advanced Photon Source, Argonne National Laboratory, Argonne, IL 60439, USA*

High-pressure x-ray emission measurements are used to decide the longstanding debate over the nature of the isostructural ( $\alpha$ ,  $\gamma$ ) volume collapse in elemental cerium. Extended local atomic model calculations show that the satellite of the  $L\gamma$  emission line offers direct access to the total angular momentum observable  $\langle J^2 \rangle$ . This satellite experiences a 30% step-like decrease across the volume collapse, validating the Kondo model in conjunction with previous measurements. Direct comparison is made with previous predictions by dynamical mean field theory. A general experimental methodology is demonstrated for analogous work on a wide range of strongly correlated f-electron systems.

PACS numbers: 64.70.K-, 71.27.+a, 71.30.+h, 71.10.-w

\* Corresponding author: [bradley41@llnl.gov](mailto:bradley41@llnl.gov)

Despite decades of work, a coherent, *ab-initio* understanding of *f* electrons in condensed matter remains elusive. Much of this difficulty stems from the nature of both *4f* and *5f* states: they exhibit a large density of states near the Fermi energy, are capable of both localized and itinerant character, and often feature multiple low lying “ground” states that are nearly degenerate. Accordingly, understanding the electronic interactions that determine the exotic behavior in these systems is challenging. A particularly striking example is elemental Ce metal, which has served as a testing ground for state-of-the-art theoretical models treating its fascinating behavior under pressure: a large volume collapse (VC) of  $\sim 14\%$  at room temperature terminating in a critical point at  $\sim 470$  K and 1.5 GPa [1, 2]. The two latest theoretical models, the Hubbard Mott (HM) [3] and the Kondo VC (KVC) [4-6] both attempt to explain the evolution of the strongly correlated *f*-electrons across this transition. In this letter, we will show that experimentally probing the ‘bare’ atomic moment ( $\langle J^2 \rangle$ ), in conjunction with previous observations of *4f* occupation and magnetic susceptibility, can finally resolve this question for Ce. Moreover, this will demonstrate a methodology that is broadly applicable to many *f*-electron systems—a class of materials whose complex phase evolutions, often including large volume collapse, have historically been very difficult to understand.

Recently, the KVC model has been used to model the experimentally measured equation of state at different temperatures up to 800 K within experimental uncertainty [2]. However, the HM model also seems to be able to reproduce the equation of state in a similar fashion [7] and the matter stands undecided [8, 9]. Provocative work in support of the Kondo picture has been performed on cerium alloyed with 10 at.% scandium at 140 K

by Murani *et al.* [10]. However, it has been argued that the electron interactions in a 10% alloy are quite different from the pure element and disturb the  $f$  electrons, as has been found for other materials [11, 12]. However, the HM model predicts that the transition temperature varies linearly with pressure [13] as experimentally observed [14] while the p-T locus of the VC in the Kondo model exhibits a significant curvature [6]. Also, the HM model relies on only one adjustable parameter, the energy shift between the two phases [7]. Local density approximation calculations (LDA) combined with dynamical mean field theory (DMFT) are generally in support of the Kondo screening mechanism for Ce [15 -18]. For example, Rueff *et al.* [19] used resonant XES and Anderson impurity model calculations to determine that  $n_f$  dropped from 0.97 (0 kbar) to 0.81 (20 kbar) across the Ce VC, in fair to satisfactory agreement with various DMFT calculations [15, 16, 20]. Furthermore, DMFT calculations have been expanded to other rare earth elements exhibiting a VC [21], prompting measurement of the pure lanthanide metals at high pressure.

While both KVC and HM theories agree in many aspects, they disagree strongly in their expectations of the behavior of the  $4f$  moment across the VC. The HM model expects the localized  $4f$ -state of the  $\gamma$ -phase to transform into a weakly correlated  $4f$  band in the  $\alpha$ -phase resulting in a quenching of the intrinsic  $4f$  moment [3]. On the other hand, the KVC model predicts a dramatic change in dynamic screening of the intrinsic  $4f$  moment through an exponential rise of the Kondo temperature with decreasing volume, reflected in a rapid drop in entropy from the  $\gamma$ - to the  $\alpha$ -side [15,20]. Though physically quite different, both theories effectively explain the measured differences in the time-averaged magnetic properties of the two phases: the  $\gamma$ -phase exhibits para-magnetism of

the Curie-Weiss type, and the magnetic susceptibility drops across the VC to values that are more in line with a strongly enhanced Pauli-paramagnetism [14, 22, 23].

Therefore, only a measurement of the intrinsic (or instantaneous) magnetic moment per  $4f$  electron (i.e.  $\langle J \rangle$ ), can differentiate between the two models. It is this critical quantity we investigate here with X-ray emission spectroscopy (XES). We show that experimentally probing the ‘bare’ atomic moment ( $\langle J \rangle$ ), in conjunction with previous observations of  $4f$  occupation and magnetic susceptibility, finally resolves this question for Ce. Moreover, as we demonstrate below, an independent, experimentally determined  $n_f$ , though not itself a determination of the moment, contributes an important baseline for interpreting the present XES results in terms of  $\langle J \rangle$ .

Here we present critical new evidence, directly validating the KVC, using high-pressure non-resonant x-ray emission spectroscopy (NXES) combined with a modified atomic calculation of elemental Ce. This modified-atomic model reproduces the data quite well, allowing us to clearly articulate the meaning of the spectral changes that occur during the VC. We find that the experiment indicates a sudden onset of  $4f$ -to-conduction-band hybridization concomitant with the volume collapse, which is consistent with the Kondo hypothesis. More importantly, the experiment shows that in the collapsed phase, there is a persistent instantaneous magnetic moment per  $4f$  electron. When coupled with the previously observed drop in magnetic susceptibility over the volume collapse, this persistent moment confirms the existence of the Kondo screening mechanism. Finally, we relate our experimental results to explicit, quantitative predictions of the total angular momentum ( $\langle J^2 \rangle$ ) and the number of  $4f$  electrons ( $n_f$ ) made by recent DMFT calculations, arguing that considerable open questions remain about the evolution of these

observables. This last result is especially striking given that these calculations have enjoyed a spate of recent successes for *f*-electron materials, such as Ce [19], Pr [24] and Gd [25] as well as actinides such as Pu [26, 27] and Am [28,29].

The Ce  $L\gamma$  NXES experiments were performed at beamline 16IDD of the High Pressure Collaborative Access Team (HPCAT) at the Advanced Photon Source. Samples were pressurized through membrane-driven diamond anvil cells (DACs) and great care was taken to maintain a pure Ce metal sample inside the DACs, as reported elsewhere [2, 24]. High energy x-rays ( $\sim 18$  keV) were incident through the diamonds, and the outgoing  $L\gamma$  x-rays were recorded by scanning a standard four-inch, spherically-bent (333) Si analyzer crystal that was placed at 90 degrees to the beam to capture photons leaving through a 3mm diameter Be gasket (0.25 eV per step, 1 eV resolution).

The spectra were calculated with a treatment specifically developed for this data — a ‘modified-atomic’ approach explicitly including the proper atomic physics necessary to describe the deep core-hole spectroscopy [30, 31]. Our model for Ce includes the electron-electron interactions between the  $4f$ ,  $3d$ , and  $2p$  electrons, which are involved in the NXES process as described below but also give rise to, for example, Hund’s rules. It is because of these interactions that the  $L\gamma$  spectrum has a low-energy satellite feature sensitive to the *f*-electron occupancy and moment. The *f* electrons themselves respond to the external applied pressure via their hybridization with higher energy conduction orbitals, but this hybridization is by definition not included in a pure atomic calculation. Therefore, we have extended the local atomic model in analogy with the Anderson impurity model: each of the seven valence *f* orbitals is allowed to hybridize with five effective conduction orbitals. The number of orbitals included in the calculation (three

2*p*, five 3*d*, seven 4*f* and five conduction) must remain small because the interactions are treated explicitly via the exact-diagonalization numerical technique, and thus the computational cost increases exponentially with the number of orbitals. Using hybridization to extend the atomic model in this way is similar to the inclusion of explicit ligand atoms, which has proven useful in modeling the spectroscopy of transition-metal and rare-earth oxides in strongly-correlated *d*-electron systems under pressure [32, 33]. The parameters of our model are consistent with previous work [6]. We set the 4*f*-orbital energy 0.8 eV below the conduction orbital energy; the hybridization *V* is varied from 0.0 to 0.2 eV; and the interaction parameters (orbital dependent Coulomb *U*) are calculated from the Racah parameters given in the output of Cowan’s code [34]. The spectra are simulated using the Kramers-Heisenberg formula [35].

In Figure 1a, we present the experimental  $L\gamma$  NXES data and the predictions from our extended local atomic model, demonstrating that the atomic treatment captures the spectrum quite well. The experiment shows a main emission line near 6052 eV emission energy for the  $4d_{3/2} \rightarrow 2p_{1/2}$  transition as well as a satellite feature around 6034 eV. The satellite emanates from a large number of features split into atomic multiplets derived from the electron-electron interactions between the 4*f*, 3*d*, and 2*p* electrons. The sharpness of the satellite feature in the calculation, compared to the experiment, comes from the fact that the 4*f* electrons are allowed to hybridize with five discrete conduction orbitals, rather than with a broad 5*d* band as in the real metal. The closeup in figure 1c shows that a step-like decrease in the satellite accompanies the Ce  $\gamma \rightarrow \alpha$  volume collapse at  $\sim 9$  kbar in the experimental spectra. Figure 1c also shows that this behavior is successfully modeled by the onset of hybridization between the 4*f* orbitals and higher

lying  $d$ -type states. This yields our first main result: the pressure dependence of the  $L\gamma$  spectrum shows  $4f$ -to- $d$  hybridization—a key aspect of the Kondo model.

In figure 1b, we demonstrate that the Ce  $L\gamma$  measurement is a means of evaluating the “bare” atomic  $4f$  moment  $\langle J \rangle$ . The bare or instantaneous moment is an especially important observable, because in the Kondo picture the  $4f$  moments are dynamically screened by  $d$ -band electrons—a mechanism invoked to explain the sharp reduction in the magnetic susceptibility of Ce in the collapsed phase without resorting to fully delocalized  $4f$  states, as in the Mott picture. It was expected that the  $L\gamma$  x-ray emission measurement would “see” past the Kondo screening and probe the angular momentum of the atomic-like  $4f$  orbitals. In Figure 1b, we show that this is indeed confirmed by our calculations: As the  $f$ - $d$  hybridization is increased, the satellite intensity and the expected value of the bare atomic moment (shown in terms of  $\langle J^2 \rangle$ ) are predicted to decrease concurrently. The satellite intensity actually shrinks somewhat faster than the moment. The analogous measurement for transition metal systems,  $K\beta$  emission spectroscopy, is commonly used to evaluate  $3d$  moments [36, 37], and this work opens the door for use of the  $L\gamma$  line as an indicator of the bare atomic moment in rare earth materials, via suitable experimental standards.

With this in mind, turning back to the data in Figure 1c, we now see that there is a measured decrease in the instantaneous  $4f$  moment as Ce progresses through the volume collapse. This puts us in the potentially confusing position of validating the Kondo hypothesis by observing greater  $f$ - $d$  mixing, but also observing a lowering of the magnetic moment typically associated with a Mott-like orbital delocalization. The resolution of this apparent conflict lies in considering the number of  $f$  electrons per site ( $n_f$ ) in our enhanced

local atomic model, fractional changes of which precisely track fractional changes in the observed moment. As the  $f$ - $d$  hybridization parameter is increased, the  $f$  electrons are mixed out of their native orbitals and the instantaneous moment drops in proportion to  $n_f$ . Put in multi-configurational language, the  $4f^0$  component of the wavefunction turns on sharply with the volume collapse, and is weighted more than the  $4f^2$  component, which would drive the satellite peak higher. This “collapse” of the moment does not indicate a strong change in the  $\langle J^2 \rangle$  per  $4f$  electron, instead it indicates decreased occupancy, as seen previously [19].

With this understanding of the measurement, it becomes clear that these results constitute a direct observation of Kondo screening in Ce: While the magnetic susceptibility is known to drop by ~80% (from  $22 \cdot 10^{-4}$  emu/mole to  $5 \cdot 10^{-4}$  emu/mole) [22, 23], the “instantaneous moment” (i.e.  $\langle J \rangle$ ), per  $4f$  electron, is here observed to be relatively stable through the collapse. This means the larger drop in susceptibility is not due to intrinsic changes in the  $4f$  localization, but is instead a dynamic effect—i.e. the conduction electron screening predicted in the Kondo picture.

We can also make a direct comparison with state-of-the-art dynamical mean-field theory calculations on Ce. To do so, we extract the pressure dependence of the integrated satellite intensity, as shown in figure 2. The data points show the satellite intensity with a thick line as a guide for the eye. The sudden change in the satellite is evident at ~9 kBar as Ce undergoes the volume collapse transition. The connection to the DMFT calculation is also shown in figure 2. As discussed above, both  $\langle J^2 \rangle$  and  $n_f$  are reflected in the satellite intensity, so previous predictions by DMFT of these quantities are plotted in figure 2 as well [21, 38]. Fractional changes in the feature intensity,  $\langle J^2 \rangle$  and  $n_f$  are

plotted on the same scale. The large change in satellite intensity ( $\sim 30\%$ ) argues that the physics of the volume-collapse transition is dominated by a decrease in  $n_f$ , and that any rise in the double occupancy configuration is relatively minor. This is in contrast to DMFT calculations, which predict a small change in  $n_f$  and a significant rise in the bare magnetic moment due to growth in the double-occupancy configuration [21,38], as shown here. DMFT, however, has been successful in predicting a large decrease in the *screened* moment [38] comparable to the collapse of the magnetic susceptibility measured experimentally [22, 23].

In conclusion, we have presented experimental results from high-pressure NXES on elemental Ce metal, along with a new, modified-atomic treatment to simulate the spectra. This experiment-theory combination allows us to present direct evidence in strong support of the Kondo hypothesis of the Ce isostructural ( $\gamma$ - $\alpha$ ) volume collapse transition. In addition to dealing with this specific, long-argued scientific question, this work also contributes within the larger context of strongly-correlated condensed-matter physics by (1) exhibiting a program of study relevant for many f-electron systems and (2) providing a direct evaluation of observables calculated by DMFT. While previous efforts by these authors and others have shown that DMFT is exceptionally well suited to these systems and quantitatively predictive, especially in terms of multi-configurational occupancy weights, this work exhibits an exciting challenge for the development of the treatment of magnetism in strongly correlated systems.

## **Acknowledgements**

This work has been supported by the LDRD 07-ERD-029 and 12-LW-014 at LLNL and was performed under the auspices of the U.S. Department of Energy by Lawrence

Livermore National Laboratory in part under contract W-7405-Eng-48 and in part under Contract DE-AC52-07NA27344.

The x-ray work was performed at beam-line 16IDD of the HPCAT at the Advanced Photon Source (APS), Argonne National Laboratory. HPCAT is supported by CIW, CDAC, UNLV and LLNL through funding from DOE-NNSA, DOE-BES and NSF. APS is supported by DOE-BES, under Contract No. DE-AC02-06CH11357. The authors would like to thank A.K. McMahan for a critical reading of an earlier manuscript and many very valuable discussions and suggestions.

### References:

- [1] F. Decremps, L. Belhadi, D.L. Farber, K.T. Moore, F. Occelli, M. Gauthier, A. Polian, D. Antonangeli, C.M. Aracne-Ruddle, and B. Amadon, *Phys. Rev. Lett.* **106**, 065701 (2011).
- [2] M.J. Lipp, D. Jackson, H. Cynn, C. Aracne, W.J. Evans, and A.K. McMahan, *Phys. Rev. Lett.* **101**, 165703 (2008).
- [3] B. Johansson, *Philos. Mag.* **30**, 469 (1974). B. Johansson, *Phys. Rev. B* **11**, 2740 (1975).
- [4] J. W. Allen and R. M. Martin, *Phys. Rev. Lett.* **49**, 1106 (1982).
- [5] M. Lavagna, C. Lacroix, and M. Cyrot, *Phys. Lett.* **90A**, 210 (1982).
- [6] J. W. Allen and L. Z. Liu, *Phys. Rev. B* **46**, 5047 (1992).
- [7] B. Johansson, A.V. Ruban, and I.A. Abrikosov, *Phys. Rev. Lett.* **102**, 189601 (2009), comment.
- [8] G. Kotliar, S. Y. Savrasov, K. Haule, V. S. Oudovenko, O. Parcollet, and C. A. Marianetti, *Rev. Mod. Phys.* **78**, 865 (2006).
- [9] K. T. Moore and G. van der Laan, *Rev. Mod. Phys.* **81**, 235 (2009).
- [10] A.P. Murani, S.J. Levett, and J.W. Taylor, *Phys. Rev. Lett.* **95**, 256403 (2005).
- [11] J.-P. Rueff, *Rev. Mod. Phys.* **82**, 847 (2010).
- [12] E. Vescovo, L. Braicovich, B. De Michelis, A. Fasana, R. Eggenhöfner, G. Iandelli, G. L. Olcese, and A. Palenzona, *Phys. Rev. B* **43**, 12281 (1991).
- [13] B. Johansson, I.A. Abrikosov, M. Aldén, A.V. Ruban, and H.L. Skriver, *Phys. Rev. Lett.* **74**, 2335 (1995).
- [14] D.C. Koskenmaki and K. A. Gschneidner, Jr., *Handbook on the Physics and Chemistry of Rare Earths*, chap. 4, p.337 (North- Holland Publishing Company, Amsterdam, 1978).
- [15] A. K. McMahan, K. Held, and R. T. Scalettar, *Phys. Rev. B* **67**, 075108 (2003).
- [16] M. B. Zöfl, I. A. Nekrasov, Th. Pruschke, V. I. Anisimov, and J. Keller, *Phys. Rev. Lett.* **87**, 276403 (2001).
- [17] K. Held, A. K. McMahan, and R. T. Scalettar, *Phys. Rev. Lett.* **87**, 276404 (2001).
- [18] K. Haule, V. Oudovenko, S. Y. Savrasov, and G. Kotliar, *Phys. Rev. Lett.* **94**, 036401 (2005).

- [19] J.-P. Rueff, J.-P. Itie, M. Taguchi, C.F. Hague, J.-M. Mariot, R. Delaunay, J.-P. Kappler, and N. Jaouen, *Phys. Rev. Lett.* **96**, 237403 (2006).
- [20] B. Amadon, S. Biermann, A. Georges, and F. Aryasetiawan, *Phys. Rev. Lett.* **96**, 066402 (2006).
- [21] A. K. McMahan, *Phys. Rev. B* **72**, 115125 (2005).
- [22] M.R. MacPherson, G.E. Everett, D. Wohlleben, and M.B. Maple, *Phys. Rev. Lett.* **26**, 20 (1971).
- [23] T. Naka, T. Matsumoto, N. Mori, *Physica B* **205**, 121 (1995).
- [24] J. A. Bradley, K.T. Moore, M.J. Lipp, B.A. Mattern, J.I. Pacold, G. T. Seidler, P. Chow, E. Rod, Y. Xiao, W.J. Evans, *Phys. Rev. B* **85**, 100102 (2012).
- [25] B. Maddox, A. Lazicki, C.S. Yoo, V. Iota, M. Chen, A.K. McMahan, M.Y. Hu, P. Chow, R.T. Scalettar, and W.E. Pickett, *Phys. Rev. Lett.* **96**, 215701 (2006).
- [26] X. Dai, S. K. Savrasov, G. Kotliar, A. Migliori, H. Ledbetter, and E. Abrahams, *Science* **300**, 953 (2003).
- [27] J.H. Shim, K. Haule, and G. Kotliar, *Nature* **446**, 513 (2007).
- [28] J.-C. Griveau, J. Rebizant, G. H. Lander, and G. Kotliar, *Phys. Rev. Lett.* **94**, 097002 (2005).
- [29] Sergej Y. Savrasov, K. Haule, and G. Kotliar, *Phys. Rev. Lett.* **96**, 036404 (2006).
- [30] F. de Groot and A. Kotani, *Core Level Spectroscopy of Solids* (CRC Press, 2008).
- [31] J. S. Griffith, *The Theory of Transition-Metal Ions* (Cambridge University Press, 1971).
- [32] S. Wang, W. L. Mao, A. P. Sorini, C.-C. Chen, T. P. Devereaux, Y. Ding, Y. Xiao, P. Chow, N. Hiraoka, H. Ishii, Y. Q. Cai, C.-C. Kao, *Phys. Rev. B* **82**, 144428 (2010).
- [33] W. S. Lee, A. P. Sorini, M. Yi, Y. D. Chuang, B. Moritz, W. L. Yang, J.-H. Chu, H. H. Kuo, A. G. Cruz-Gonzalez, I. R. Fisher, Z. Hussain, T. P. Devereaux, Z. X. Shen, *Phys. Rev. B* **85**, 155142 (2012).
- [34] R. D. Cowan, *The Theory of Atomic Structure and Spectra* (University of California Press, 1981).
- [35] W. Schuelke, *Electron Dynamics by Inelastic X-Ray Scattering* (Oxford University Press, New York, 2007).
- [36] F. de Groot, *Chemical Reviews* **101**, 1779 (2001)
- [37] G. Peng, F. M. F. deGroot, K. Hamalainen, J. A. Moore, X. Wang, M. M. Grush, J. B. Hastings, D. P. Siddons, W. H. Armstrong, O. C. Mullins and S. P. Cramer, *J. Am. Chem. Soc.* **116**, 2914 (1994).
- [38] A. K. McMahan, *Phys. Rev. B* **80**, 235105 (2009).

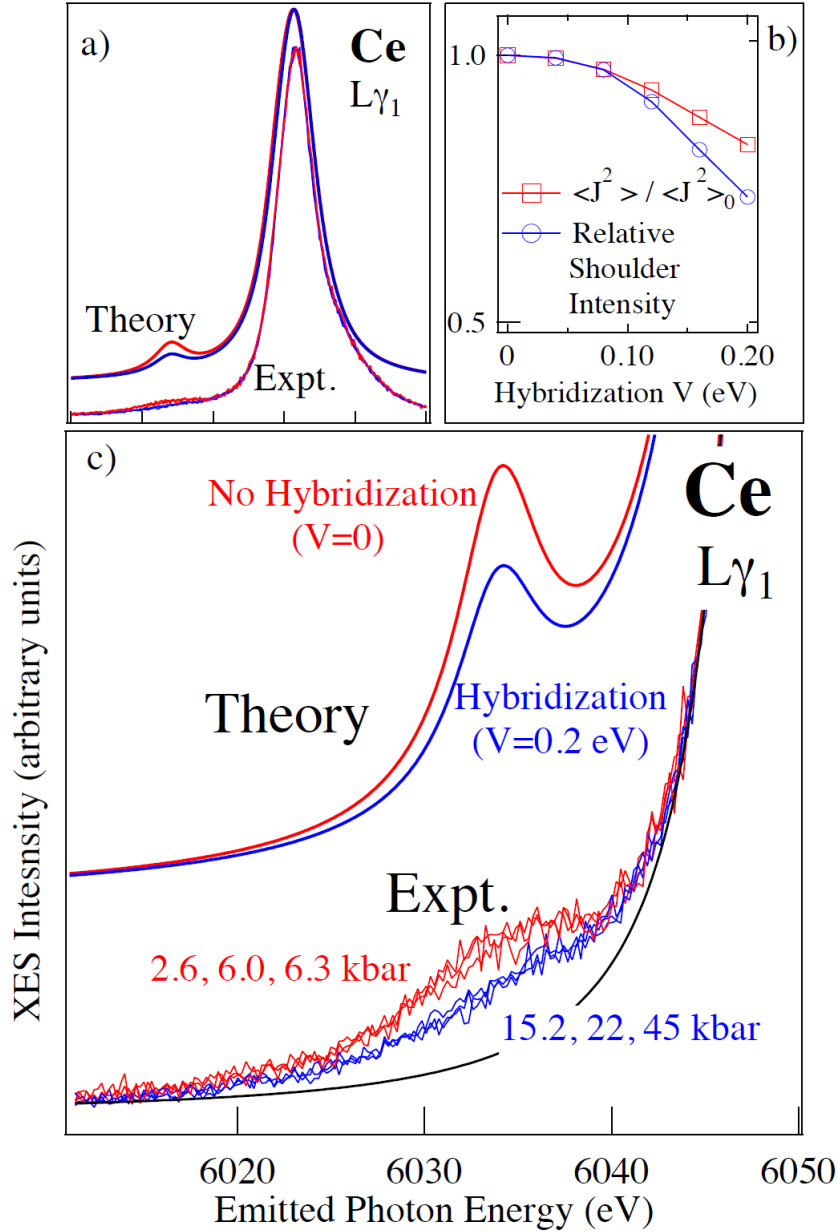


**Fig. 1** (color online):

a) The full Ce  $L\gamma_1$  emission line as measured experimentally and calculated by the extended atomic model. All theory spectra are shifted by a constant  $E_0 = 175$  eV and broadened by convolution with a 5 eV Lorentzian form.

b) Comparison of the calculated shoulder intensity of the  $L\gamma_1$  emission line with the instantaneous ("bare")  $\langle J^2 \rangle$  moment. Both decrease with growing hybridization with the shoulder intensity dropping slightly faster than the moment.

c) A close-up of the satellite region revealing the step-like nature of the volume collapse process with virtually identical lineshapes for all the pressures below the VC (2.6, 6.0 and 6.3 kbar) and – with a reduced satellite - above the VC (15.2, 22 and 45 kbar). The lines are well fit by a sum of two Lorentzians in the spectral region of interest and the black curve shows the contribution of the main peak in the shoulder region. The calculated spectra with and without hybridization (blue and red, resp.) are displayed, showing that this extension outside the atomic limit captures the spectral evolution through the volume collapse very well.

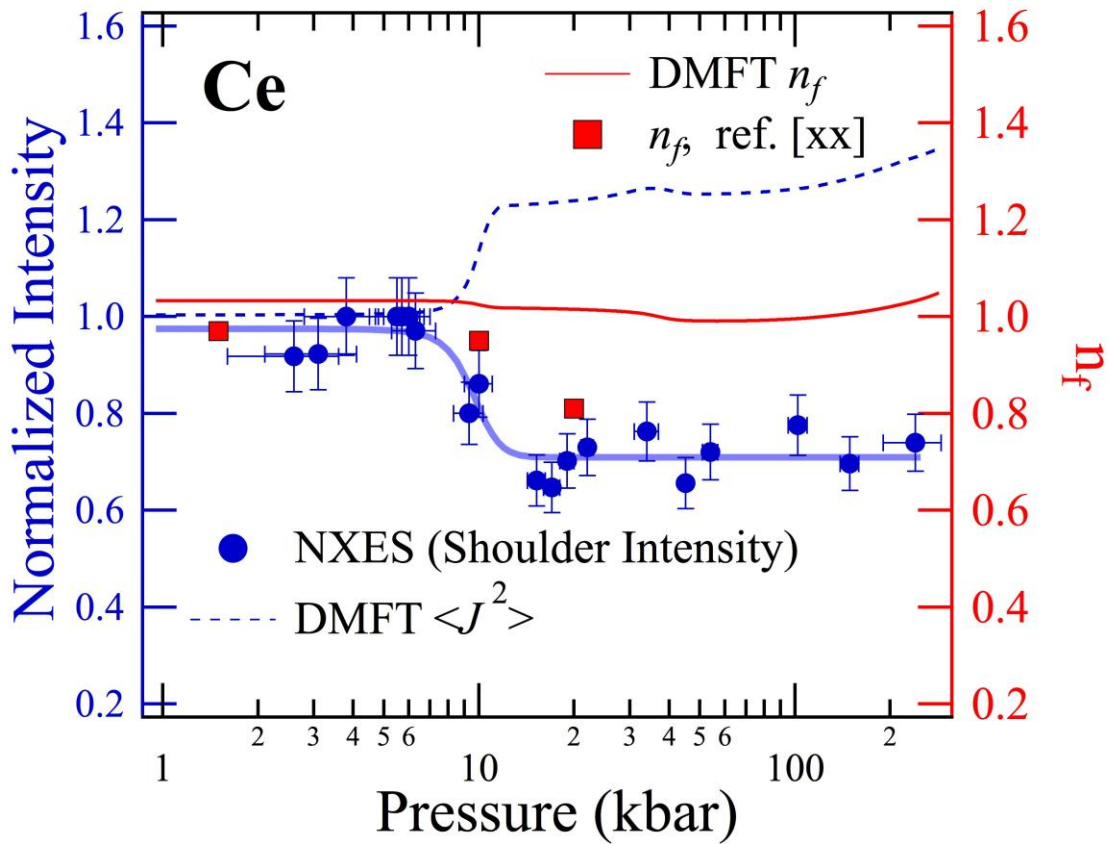


**Fig. 2** (color online):

Comparison of experimental data with DMFT predictions.

Left axis: Comparison of the normalized shoulder intensity (datapoints with error bars) with predictions for the angular quantum number  $\langle J^2 \rangle$  (dashed line), which has been normalized with regard to its atomic value. Note that the predicted  $\langle J^2 \rangle$  changes in the opposite direction than does the data. The thick line through the XES data points is a guide for the eye.

Right axis: Number of 4f electrons  $n_f$ . The previous experimental results (large squares) show a drop of 20 %, while predicted  $n_f$  (solid line) decreases only slightly across the VC. Note that the satellite intensity roughly follows the previous measurement of  $n_f$ , with the drop in intensity being slightly larger. The calculations predict this, as seen in figure 1b), where the shoulder intensity is predicted to decrease faster than  $\langle J^2 \rangle$ .